

Thiophene vs. Benzene: How π -Spacer Engineering Transforms Photocatalytic Hydrogen Evolution

Zibin Li^{a+}, Xiujuan Zhong^{a+}, Ya Chu^b, Jingkai Lin^c, Fanpeng Meng^a, Jinsheng Zhao^{a,*}, Zhengrong Wei^{d,*}, Huayang Zhang^{c,*}

^aCollege of Chemistry and Chemical Engineering, Liaocheng University, Liaocheng 252059, China.

^bSchool of Physics Science and Information Technology, Liaocheng University, Liaocheng, 252059, China.

^cSchool of Chemical Engineering, The University of Adelaide, Adelaide, SA, 5005, Australia.

^dDepartment of Physics, Hubei University, Wuhan 430062, China.

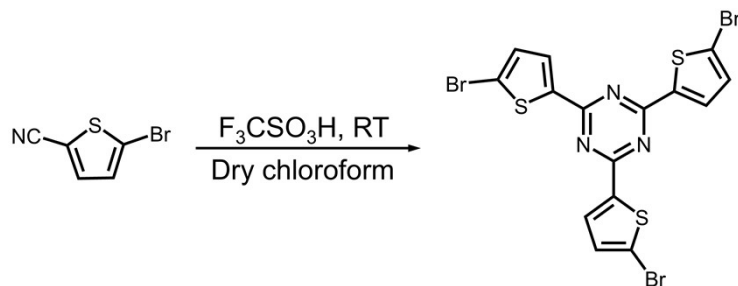
⁺The authors contribute equally to the work.

1. Experimental Section

1.1 Chemicals and Reagents

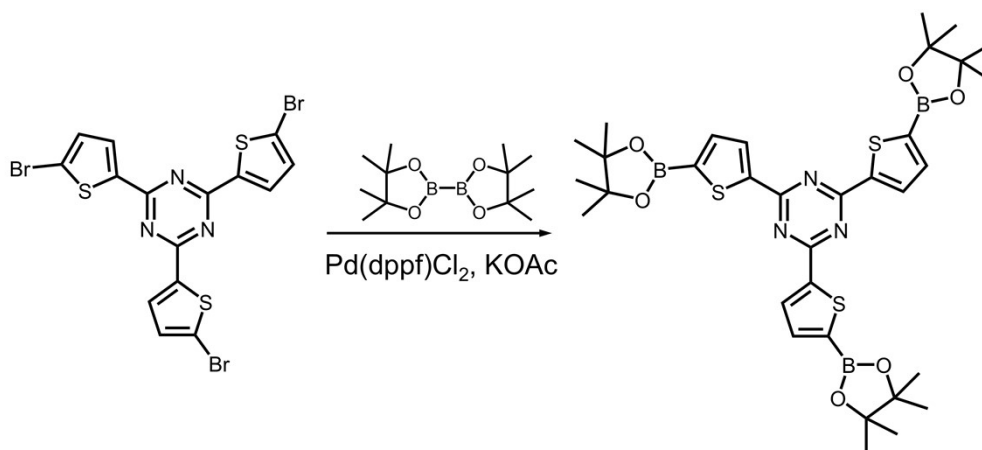
Bis(pinacolato)borane, potassium acetate, N,N-dimethylformamide (DMF), 1-Methyl-2-pyrrolidone (NMP), triethanolamine (TEOA), ascorbic acid (AA), triethylamine (TEA), acetonitrile (ACN) and isopropyl alcohol were purchased from Shanghai Aladdin Biochemical Technology Co., LTD. Pd(PPh₃)₄ was purchased from J &K Scientific. Chloroform, methanol and ethanol were purchased from Yantai Yuandong Fine Chemical Co., LTD. 5-bromothiophene-2-carbonitrile, trifluoromethanesulfonic acid, 2,4,6-tris(4-(4,4,5,5-tetramethyl-1,3,2-dioxaborolan-2-yl)phenyl)-1,3,5-triazine (M2) and 2,2',7,7'-tetrabromo-9,9'-spirobifluorene (M3) were obtained from Zhengzhou Alpha Chemical Co., LTD. 2,2,6,6-tetramethyl-1-piperidine-N-oxyl (TEMPO) and 5,5-dimethyl-1-pyrroline-N-oxide (DMPO) were obtained from Dojindo Laboratories. The above purchased samples and reagents were used without further purification.

1.2 Synthesis of 2,4,6-tris(5-bromothiophene-2-yl)-1,3,5-triazine



4.0 g (21.3 mmol) of 5-bromothiophene-2-carbonitrile was dissolved in 500 mL of dry chloroform, and 12.8 g (85.2 mmol) of trifluoromethanesulfonic acid was dropped into the solution at 0 °C. The resultant solution was magnetically stirred for 2 hours at 0 °C, and then the temperature of the solution was risen to room temperature for 48 hours. The mixture was rinsed with distilled water, and dried by anhydrous magnesium sulphate. The solution was obtained by filtration. Then, the solvent was distilled off by vacuum distillation. Finally, the crude product was purified by recrystallization in toluene to obtain a white needle solid (yield: 87.3%).

1.3 Synthesis of 2,4,6-tris(5-(4,4,5,5-tetramethyl-1,3,2-dioxaborolan-2-yl)thiophen-2-yl)-1,3,5-triazine (M1)



2.40 g of 2,4,6-tris(5-bromothiophene-2-yl)-1,3,5-triazine, 3.80 g of bis(pinacolato)borane, 1.20 g of potassium acetate, 204 mg of Pd(dppf)Cl₂ were successively added to a round bottom flask containing 70 mL of dioxane, the air in the reaction device was replaced with nitrogen, and the reaction was refluxed at 100 °C for 48 hours. After the reaction was completed and cooled to room temperature, the reaction system was poured into a beaker containing 350 mL of deionized water, extracted three times with chloroform, and the organic phases were combined. The above solution was

washed twice with saturated sodium chloride solution, dried with anhydrous magnesium sulfate, filtered and finally evaporated chloroform, the crude product obtained was purified by column chromatography with dichloromethane as eluent, and finally a yellow powder was obtained (yield: 77.5%). ^1H NMR (500 MHz, CDCl_3), δ 8.21 (d, $J = 4.0$ Hz, 3H), 7.60 (d, $J = 4.0$ Hz, 3H), 1.32 (s, 36H) (Fig. S1). ^{13}C NMR (126 MHz, CDCl_3), δ 167.92, 147.69, 137.78, 132.35, 128.56, 84.62, 24.96 (Fig. S2).

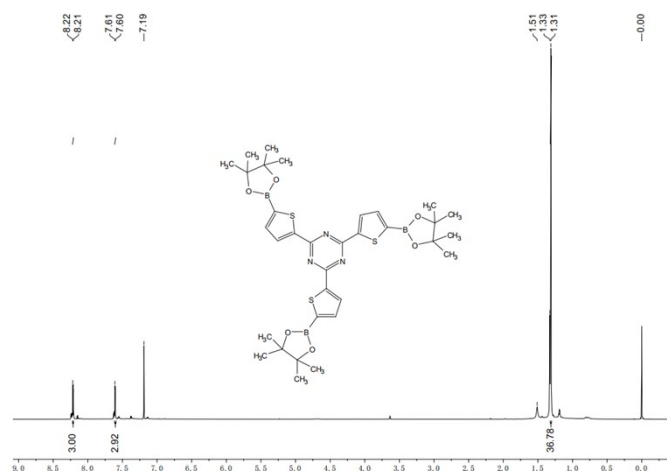


Fig. S1. ^1H NMR spectrum of M1

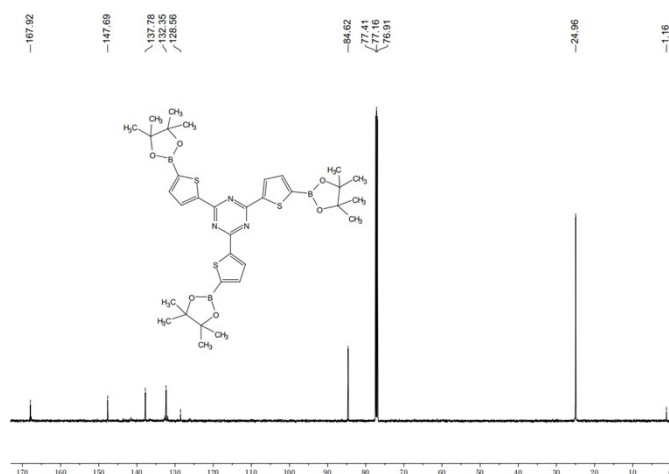


Fig. S2. ^{13}C NMR spectrum of M1

1.4 Synthesis of ThSF-CPP

Under nitrogen protection, 446.13 mg of M1, 200 mg of M3, 40 mg of $\text{Pd}(\text{PPh}_3)_4$, 12 mL of K_2CO_3 solution (2 M), and 30 mL DMF were added into a 100 mL round bottom flask. The mixture was degassed by a vacuum pump and filled back with N_2 two times. After that, the round bottom flask was heated to 130 $^\circ\text{C}$ for 48 h with stirring under the protection of N_2 atmosphere. The reaction mixture was cooled down, and the

solid produced was filtrated and washed in sequence with distilled water, ethanol, methanol, and chloroform. Then, the crude product was further purified by Soxhlet extraction with chloroform as the extraction agent. Finally, the product was dried under vacuum at 100 °C for 24 h, and the polymer ThSF-CPP was obtained as a green solid powder (yield: 89.82%). The residual Pd content of 0.27 wt% can be obtained from the ICP-MS measurement.

1.5 Synthesis of PhSF-CPP

The preparation method of PhSF-CPP was the same as that of ThSF-CPP. 434.99 mg of M2, 200 mg of M3, 40 mg of Pd(PPh₃)₄, 12 mL of K₂CO₃ solution (2 M), and 30 mL DMF were used in this polymerization. After the reaction and post-processing stages, the polymer PhSF-CPP was obtained as a gray solid powder (yield: 79.75%). The residual Pd content of 0.06 wt% can be obtained from ICP-MS measurement.

2. Characterization methods

2.1 Instrumental Information

The structural identification of polymers was fulfilled by instrumental methods including Nicolet Avatar 360 FT-IR spectrometer, Bruker Avance III HD 600 MHz NMR spectrometer. And, a Rigaku D/max 2500 X-ray advanced diffractometer with a Cu-K α radiation was used to identify the aggregation of polymers. ESCALAB 250Xi spectrometer was used to get the elements and their valence states. A Netzsch STA449C TG/DSC thermal analyzer was conducted under a nitrogen atmosphere between 20 °C and 800 °C. Scanning electron microscope (SEM) (Thermo Fisher Scientific FIB-SEM GX4) was coupled with an Energy dispersive X-ray spectrometry (SEM-EDX) to examine the morphology and the elemental distribution of the polymers. The transmission electron microscopy (TEM) was also taken to investigate the structural characterization using JEM-2100F TEM. Nitrogen isotherm adsorption-desorption was conducted at 77.3 K using ASAP 2460-3 (Micromeritics) volumetric adsorption analyzer. The UV-vis absorption spectrum was conducted on an Agilent Carry 5000 spectrophotometer (CA, USA). Photoluminescence (PL) spectra were collected on an F-7000 FL spectrophotometer. Time-resolved PL spectra were measured using a time-correlated single-photon counting system (FLS1000). The contents of residual Pd in

samples were measured by inductively coupled plasma mass spectrometry (ICP-MS) (ICAP RQ, Thermo Fisher). The Electron paramagnetic resonance spectroscopy was measured using a China instru & Quantumtech (Hefei) EPR200-Plus with continuous-wave X band frequency.

2.2 Calculation method

The frontier molecular orbital distribution and energy levels, ESP and electron-hole distribution in an excited state of PhSF-CPP and ThSF-CPP fragments are calculated by the gaussian 16 program package [1] at the B3LYP/6-31G (d, p) level. Differential charge density and Gibbs free energy change (ΔG_{H^*}) of HER, were performed under the framework of density functional theory (DFT) with the Vienna Ab-initio Simulation Package (VASP) [2]. The spin polarization projection augmented wave (PAW) method [3] and the Perdew-Burke-Ernzerhof (PBE) electron exchange-correlation function of generalized gradient approximation (GGA) [4] are used to describe the interactions between valence electrons and ionic core for all atoms. All geometries are adequately optimized until the convergence criteria for energy and force are less than 1×10^{-5} eV and 0.01 eV/Å, respectively. The Electron-hole distribution in an excited state was constructed by the Multiwfn program and Visual Molecular Dynamics (VMD) [5,6].

The definition of H atom adsorption Gibbs free energy (ΔG_{H^*}) as the following equation:

$$\Delta G_{H^*} = \Delta E_H + \Delta E_{ZPE} - T \Delta S_H$$

Where ΔE_H is H atom adsorption energy and was calculated by equation:

$$\Delta E_H = E_{(catalyst+H)} - E_{(catalyst)} - E_{H_2} / 2$$

Here $E_{(catalyst + H)}$, $E_{(catalyst)}$ are the energies of catalyst (PhSF-CPP and ThSF-CPP) with and without H atom adsorption, respectively. E_{H_2} is one hydrogen gas energy. Additionally, ΔE_{ZPE} stands for zero-point energy and was calculated from the vibration frequency. ΔS_H represents the entropy difference between the atomic hydrogen adsorbed and the gas phases and can approximately be regarded as $1/2(S_{H_2})$ (S_{H_2} is the entropy of gas phase H_2 at standard conditions).

For TD-DFT, the excited-state wavefunction is described as a linear combination of singly excited configuration functions. Each configuration function can act as an excitation configuration with a coefficient W or as a de-excitation configuration with a coefficient w' . The specific definition is as follows:

$$\begin{aligned}\rho^{\text{hole}}(\mathbf{r}) &= \rho_{\text{loc}}^{\text{hole}}(\mathbf{r}) + \rho_{\text{cross}}^{\text{hole}}(\mathbf{r}) \\ \rho_{\text{loc}}^{\text{hole}}(\mathbf{r}) &= \sum_{i \rightarrow a} (w_i^a)^2 \varphi_i \varphi_i - \sum_{i \leftarrow a} (w_i'^a)^2 \varphi_i \varphi_i \\ \rho_{\text{cross}}^{\text{hole}}(\mathbf{r}) &= \sum_{i \rightarrow a} \sum_{j \neq i \rightarrow a} w_i^a w_j^a \varphi_i \varphi_j - \sum_{i \leftarrow a} \sum_{j \neq i \leftarrow a} w_i'^a w_j'^a \varphi_i \varphi_j \\ \rho^{\text{ele}}(\mathbf{r}) &= \rho_{\text{loc}}^{\text{ele}}(\mathbf{r}) + \rho_{\text{cross}}^{\text{ele}}(\mathbf{r}) \\ \rho_{\text{loc}}^{\text{ele}}(\mathbf{r}) &= \sum_{i \rightarrow a} (w_i^a)^2 \varphi_a \varphi_a - \sum_{i \leftarrow a} (w_i'^a)^2 \varphi_a \varphi_a \\ \rho_{\text{cross}}^{\text{ele}}(\mathbf{r}) &= \sum_{i \rightarrow a} \sum_{i \rightarrow b \neq a} w_i^a w_i^a \varphi_a \varphi_b - \sum_{i \leftarrow a} \sum_{i \leftarrow b \neq a} w_i'^a w_i'^a \varphi_a \varphi_b\end{aligned}$$

In the above equation, \mathbf{r} represents the coordinate vector, φ denotes the orbital wave function, and \mathbf{i} or \mathbf{j} refers to occupied orbital indices, while \mathbf{a} or \mathbf{b} refers to unoccupied orbital indices. Accordingly, terms such as $\sum_{i \rightarrow a}$ represent summation over all excitation configurations, while $\sum_{i \leftarrow a}$ represents summation over all de-excitation configurations. The hole distribution (ρ^{hole}) and electron distribution (ρ^{ele}) are both divided into two components: the local term and the cross term.

The D_{CT} index, which measures the distance between the centroids of holes and electrons, is defined as follows:

$$\begin{aligned}D_x &= |X_{\text{ele}} - X_{\text{hole}}| & D_y &= |Y_{\text{ele}} - Y_{\text{hole}}| & D_z &= |Z_{\text{ele}} - Z_{\text{hole}}| \\ D_{CT} &= \sqrt{(D_x)^2 + (D_y)^2 + (D_z)^2}\end{aligned}$$

X_{hole} , Y_{hole} and Z_{hole} refer to the X, Y, and Z coordinates of the centroid of the hole. X_{ele} , Y_{ele} and Z_{ele} refer to the X, Y, and Z coordinates of the centroid of the electron.

2.3 Electrochemical measurements

Electrochemical impedance spectra (EIS) and Mott-Schottky plot were measured on a CHI660E (Chenhua, Shanghai) electrochemical workstation in a standard three-electrode system. The sample modified Pt-disk electrode with a diameter of 3 mm was

used as the working electrode and Pt flake and Ag/AgCl as the counter and reference electrodes, respectively. The mixture slurry was made as follows: polymer photocatalysts (10 mg), isopropyl alcohol (1 mL), and 30 μL of nafion, which was dispersed by ultrasound in a water bath for 30 min. The mixture slurry (10 μL) was dropped on the platinum plate electrode and dried under an infrared lamp before the measurements, which was used as the working electrode. EIS experiments were performed in a frequency range from 0.01 Hz to 100 kHz at 0.2 V, and Na_2SO_4 aqueous solution (0.5 M, pH=6.8) was used as the electrolyte.

2.4 Transient photocurrent measurements

The transient photocurrent responses (I-t) were measured on ZAHNER PP211 (Germany) electrochemical workstation in a standard three-electrode system, including a Pt sheet as the counter electrode (1 cm \times 1 cm), an Ag/AgCl electrode as the reference electrode, and a catalyst-modified indium tin oxide (ITO) electrode as the working electrode. The applied voltage difference on the working electrode is 1 V vs. Ag/AgCl. 0.5 M Na_2SO_4 aqueous solution was used as an electrolyte. The catalyst slurry was prepared by adding 10 mg of catalyst to a mixture solution of 1 mL isopropyl alcohol and 30 μL Nafion (5%), and the slurry was fully dispersed in an ultrasonic cleaner for 30 min before use. For the preparation of the ITO electrode, 20 μL of the above polymer slurry was coated on the ITO/glass electrode with a surface area of 1 cm \times 1 cm and dried under an infrared lamp.

2.5 AQY measurements

The apparent quantum yield (AQY) of the photocatalysts was measured with a monochromatic light obtained by using bandpass filters of 380, 420, 475, 500, and 600 nm with energy intensities of 33.7, 37.2, 55.7, 49.4, and 40.2 mW cm^{-2} , respectively. The AQY at a given wavelength was calculated by the following equation [7]:

$$AQY = 2 \frac{N_0}{N_p} \times 100\% = \frac{2 \times M \times N_A \times h \times c}{S \times P \times t \times \lambda} \times 100\%$$

Where M is the amount of H_2 (mol) produced, N_A is Avogadro constant ($6.02 \times 10^{23} \text{ mol}^{-1}$), h is the Planck constant ($6.626 \times 10^{-34} \text{ J} \cdot \text{s}$), c is the speed of light in vacuum ($3 \times 10^8 \text{ m/s}$), S is the irradiation area (19.6 cm^2 in our experiment), P is the intensity of

irradiation light (W/cm^2), t is the irradiation time (s), λ is the wavelength of the monochromatic light (m).

2.6 Photocatalytic hydrogen evolution experiment

All the photocatalytic experiments were carried out in an all-glass automatic online trace gas analysis system (CEL-PAEM-D8, Beijing China Education Au-Light Technology Co., LTD.). First of all, 10 mg of polymer, 10.56 g of AA, 10 mL of NMP, and 46 mL of distilled water were added to a 100-mL Pyrex glass reaction vessel, and then 4 mL of NaOH solution (5 M) was added to adjust the pH of the mixed solution to 4. Afterwards, the mixture is sonicated for 20 min to obtain a uniformly dispersed suspension, and then 12 μL of chloroplatinic acid (3 wt%) as cocatalyst was added into solution. The system was degassed for half an hour to remove the dissolved oxygen, the suspension was irradiated with a 300 W Xe lamp and stirred (with or without a UV cutoff filter ($\lambda > 420 \text{ nm}$)). The light intensities were measured to be 590 mW cm^{-2} under full arc light and 302 mW cm^{-2} under visible light. The reaction unit is kept at a temperature of $10 \text{ }^\circ\text{C}$ with a circulating water cooling system. The hydrogen evolution was monitored using gas chromatography (CEAULIFGT, GC-7920) with a TCD detector every 0.5 h, which used a TDX-01 column, argon as the carrier gas, and a column oven temperature of $80 \text{ }^\circ\text{C}$. The stability test was conducted by recovering the photocatalyst through filtration after each cycle, resuspending it in fresh medium, and repeating the above operation for a determined number of cycles.

Fig. S3. PXRD pattern (a) and TGA curves (b) of the polymers.

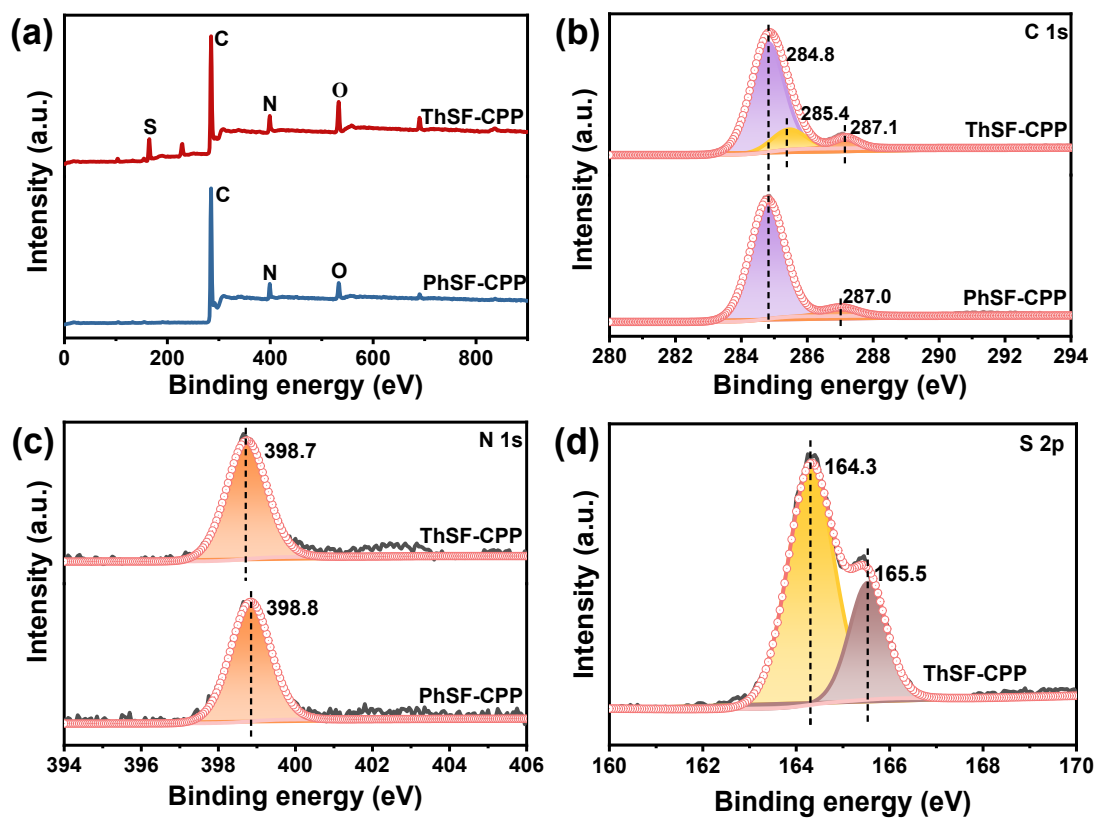


Fig. S4. XPS survey spectrum (a), high-resolution XPS spectra of C 1s region (b), N 1s region (c) and S 2p region (d) of the polymers.

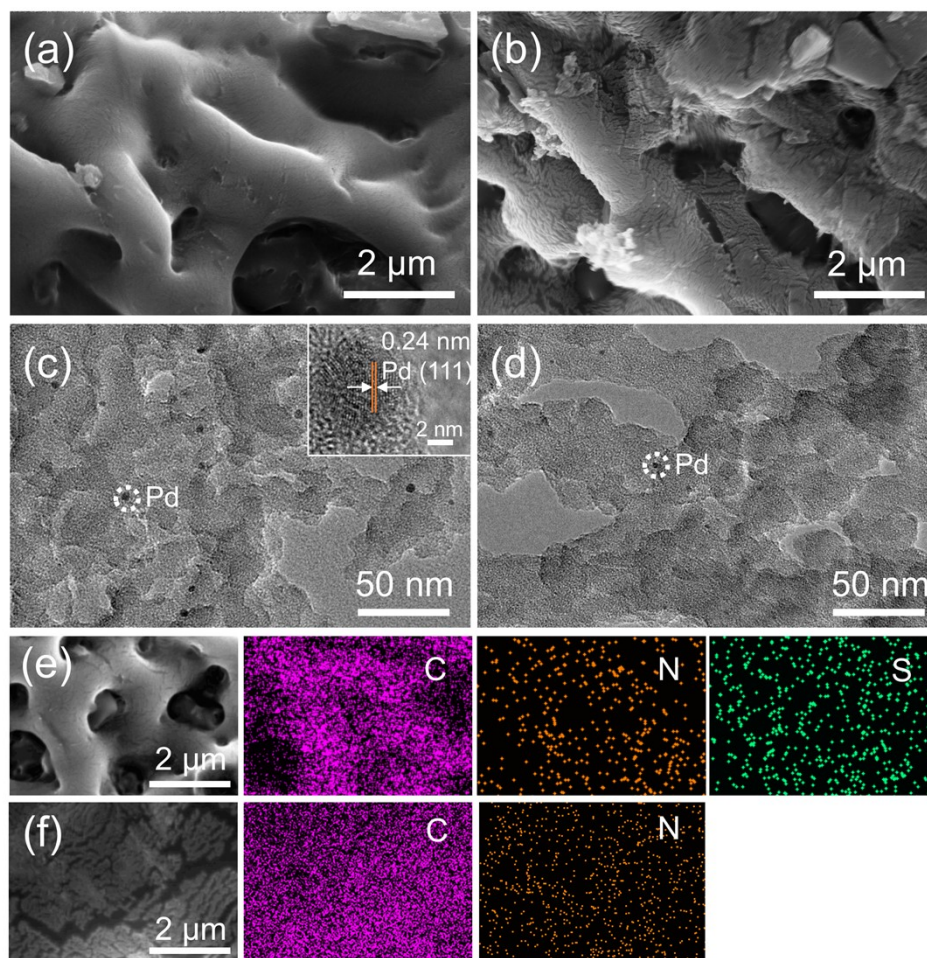


Fig. S5. SEM images of ThSF-CPP (a) and PhSF-CPP (b). TEM images of ThSF-CPP (c) and PhSF-CPP (d). EDX element mapping images for ThSF-CPP (e) and PhSF-CPP (f).

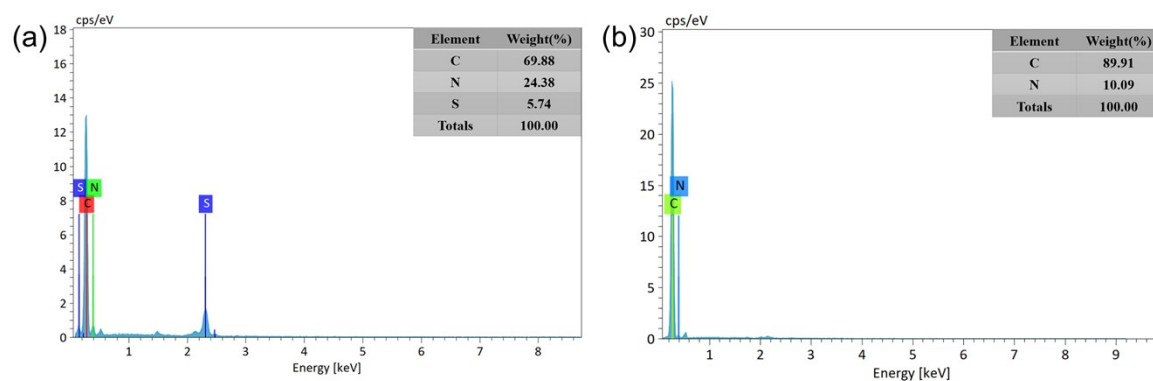


Fig. S6. EDX images of ThSF-CPP (a) and PhSF-CPP (b).

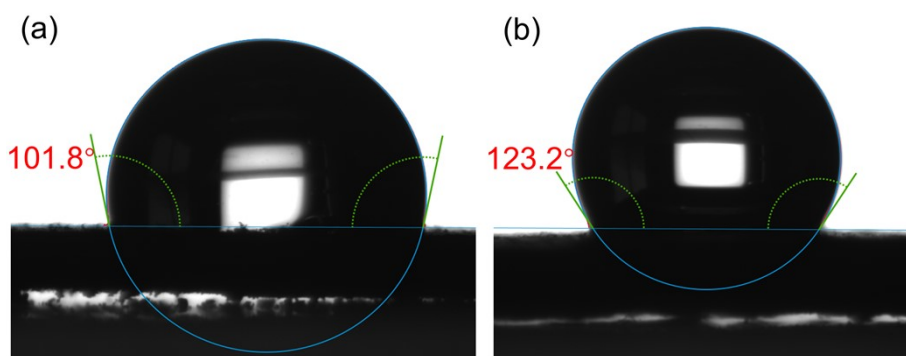


Fig. S7. Water contact angles of ThSF-CPP (a) and PhSF-CPP (b).

Fig. S8. N_2 adsorption–desorption isotherms of ThSF-CPP (a) and PhSF-CPP (b) at 77 K. Pore size distribution was shown in the inset.

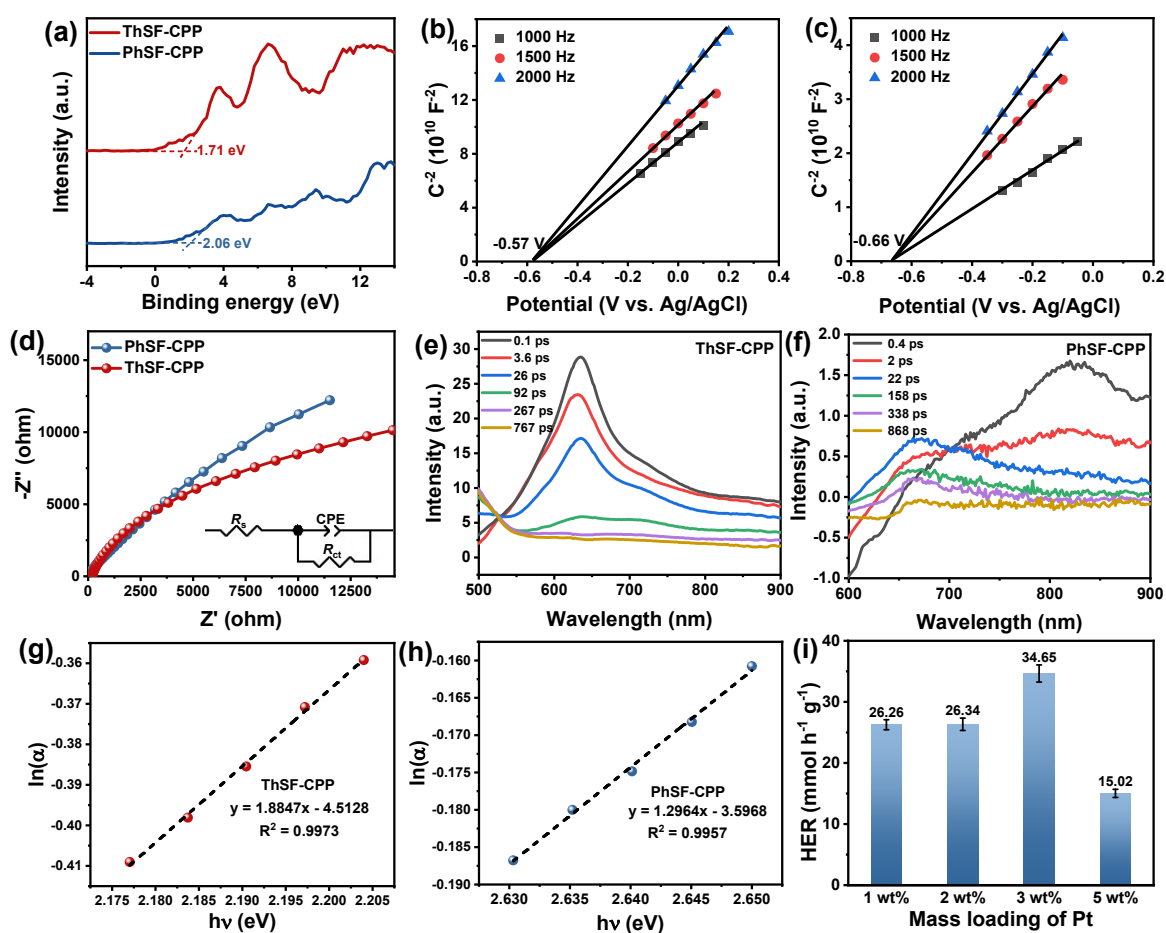


Fig. S9. VB-XPS spectra (a) of the polymers. Mott-Schottky plots of ThSF-CPP (b) and PhSF-CPP (c). Nyquist impedance plot (d) of the polymers. Fs-TA spectra of ThSF-CPP (e) and PhSF-CPP (f). Urbach energy plot of ThSF-CPP (g) and PhSF-CPP (h). HERs of ThSF-CPP with different Pt contents (i) under full arc light.

Table S1. The specific parameters of the main component in the equivalent circuit diagram

Photocatalyst	ThSF-CPP	PhSF-CPP
---------------	----------	----------

R_s	53.81 Ω	41.19 Ω
R_{ct}	18413 Ω	36617 Ω

Table S2. Photocatalytic hydrogen evolution performance of the reported organic photocatalysts

Photocatalyst	Cocatalyst	Sacrificial agent	HER (mmol g ⁻¹ h ⁻¹)	AQY (%)	Refs
SP-CMP	No	TEA	1.15 ($\lambda > 295$ nm)	0.23 (420 nm)	8
S-CMP3	No	TEA	6.08 ($\lambda > 295$ nm)	—	9
TBT-BDT	3 wt% Pt	TEOA	4.2 ($\lambda > 400$ nm)	—	10
TEBN11	3 wt% Pt	TEA	1.89 ($\lambda > 420$ nm)	—	11
Py-TPT-CMP	No	TEA	10.81 ($\lambda > 380$ nm)	41.9 (420 nm)	12
CMP-Tz	3 wt% Pt	AA	3.21 ($\lambda > 420$ nm)	1.59 (450 nm)	13
SNP-BTT1	3 wt% Pt	TEOA	3.16 ($\lambda > 395$ nm)	4.5 (420 nm)	14
Zn-Por-TPT	2 wt% Pt	AA	11.45 ($\lambda > 380$ nm)	2.53 (420 nm)	15
ThSF-CPP	3 wt% Pt	AA	34.65 ($\lambda > 300$ nm)	7.3 (475 nm)	This work

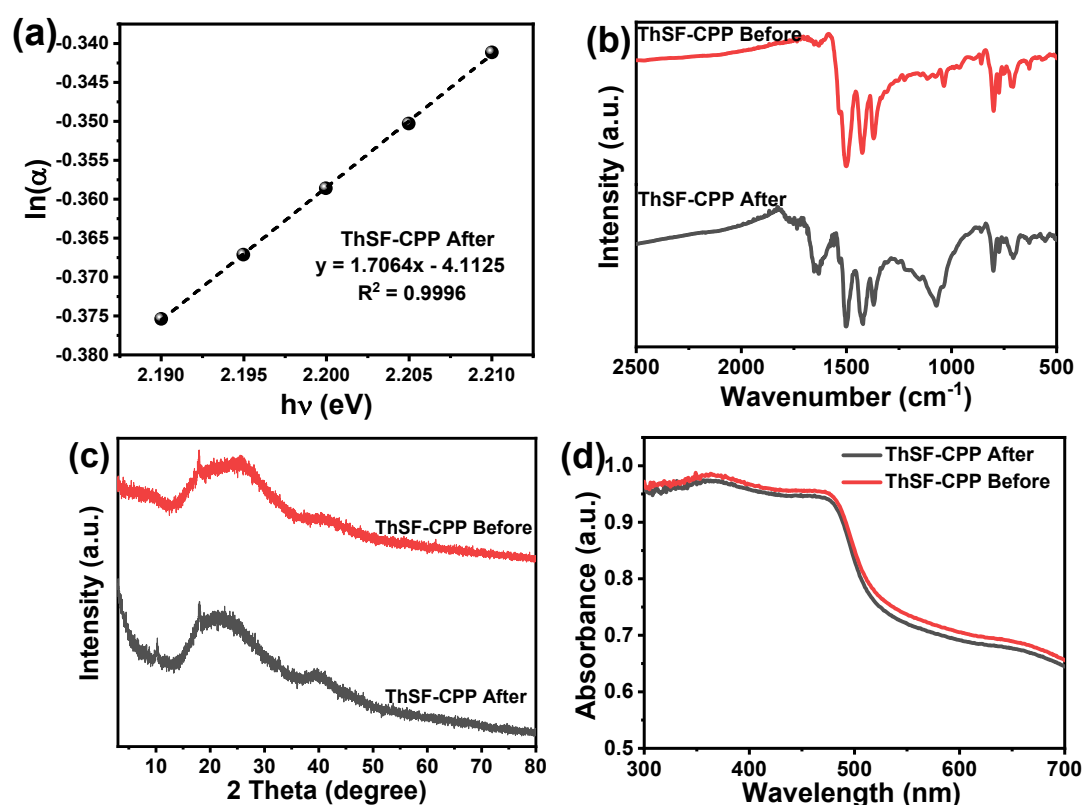


Fig. S10. Urbach energy plot of ThSF-CPP after irradiation under full-spectrum irradiation (a). FT-IR spectra (b), PXRD patterns (c) and UV-vis absorption spectrum (d) of ThSF-CPP before and after irradiation under full-spectrum irradiation.

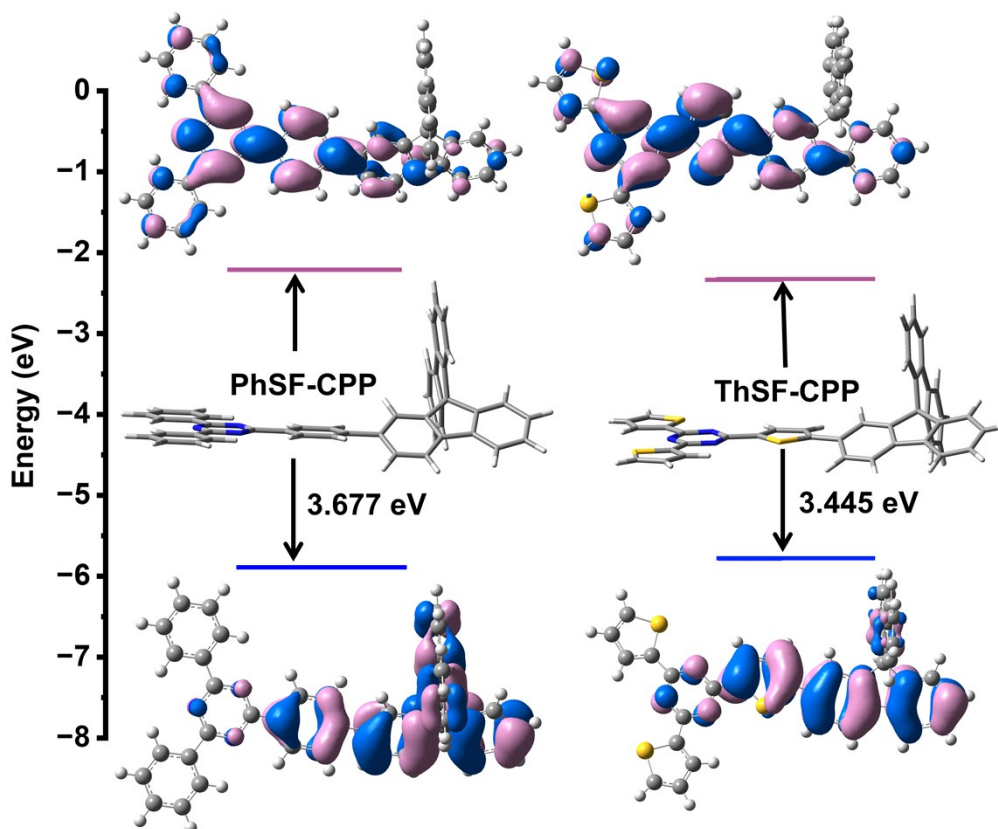


Fig. S11. Frontier Molecular orbital and HOMO-LUMO energy of fragment of PhSF-CPP and ThSF-CPP.

Table S3. Information of the first five excited states for PhSF-CPP fragment from TD-DFT calculation.

Excited State	Excitation energy (eV)	Excitation wavelength (nm)	Oscillator strength
1	4.0856	303.46	1.5738
2	4.5021	275.39	0.0018
3	4.5815	270.62	0.0007
4	4.5832	270.52	0.0002
5	4.6187	268.44	0.0059

Table S4. Information of the first five excited states for ThSF-CPP fragment from TD-DFT calculation.

Excited State	Excitation energy (eV)	Excitation wavelength (nm)	Oscillator strength
1	3.6247	342.06	1.5015
2	4.2664	290.60	0.0009
3	4.4045	281.49	0.6369
4	4.5097	274.93	0.0092
5	4.5902	270.11	0.0000

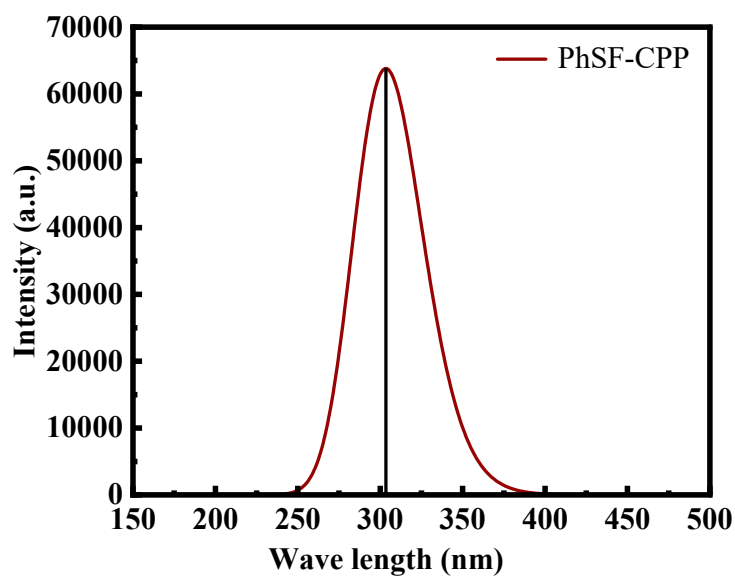


Fig. S12. The UV visible absorption spectrum of PhSF-CPP fragments calculated by TD-DFT.

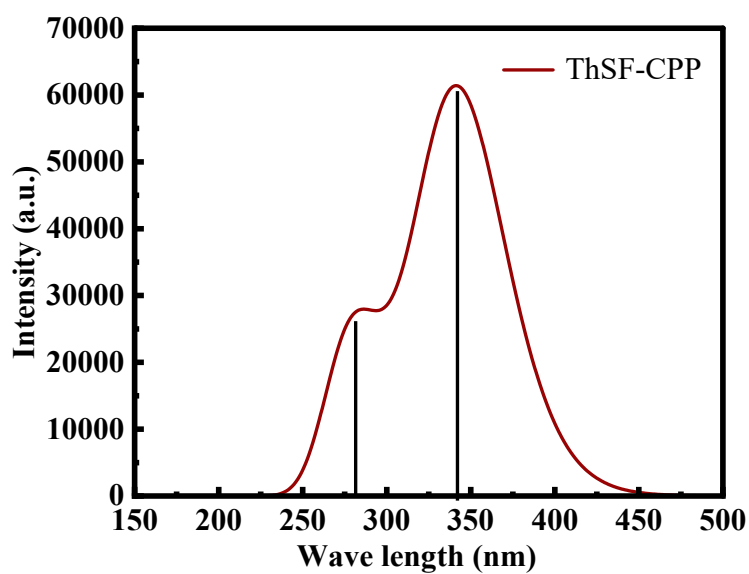


Fig. S13. The UV visible absorption spectrum of ThSF-CPP fragments calculated by TD-DFT.

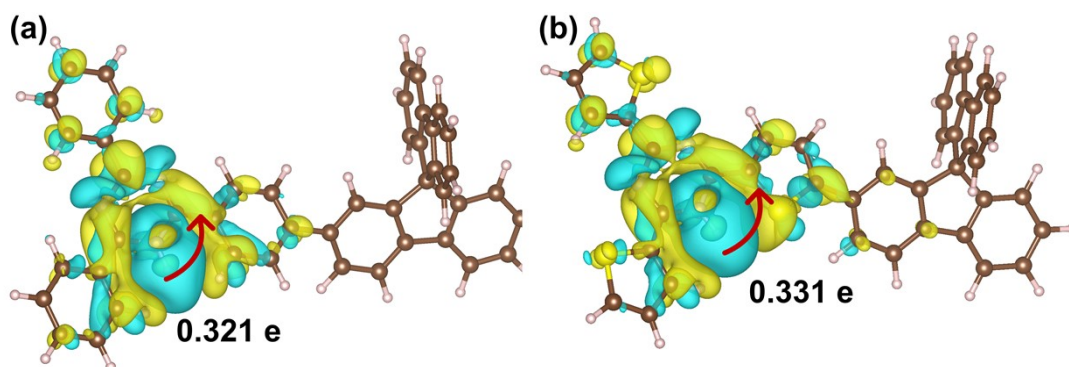


Fig. S14. The charge density differences of H chemisorbed on PhSF-CPP (a) and ThSF-CPP (b). cyan and yellow represent charge depletion and accumulation, respectively. The isosurface value is 0.003 e/Å³.

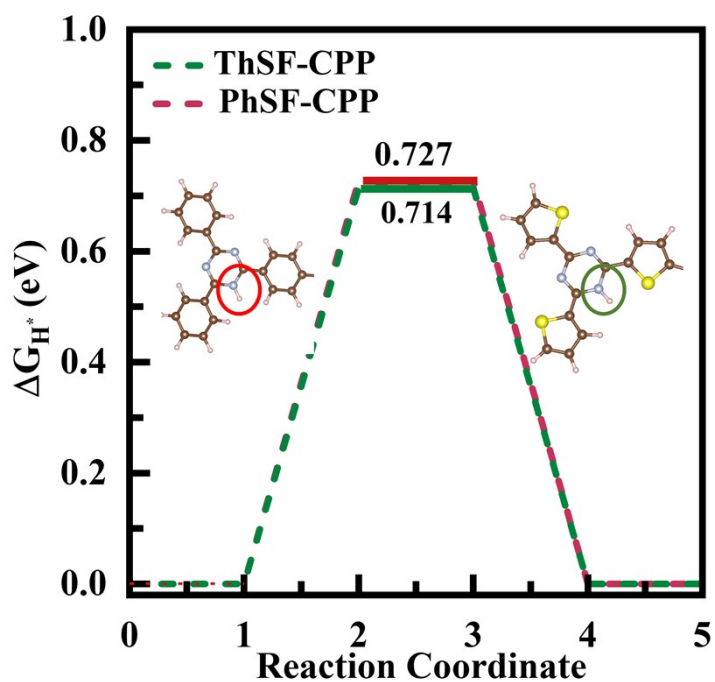


Fig. S15. The calculated hydrogen evolution reaction energy profile of PhSF-CPP and ThSF-CPP.

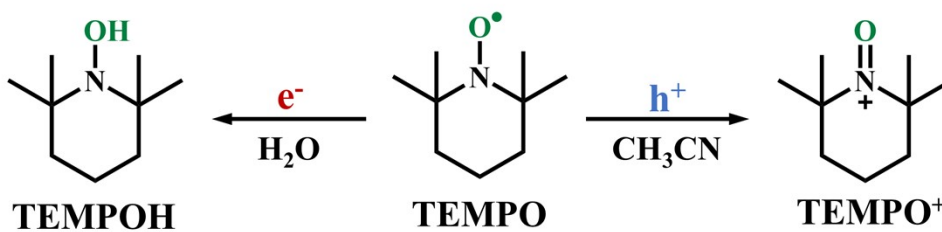


Fig. S16. Trapping mechanism of TEMPO.

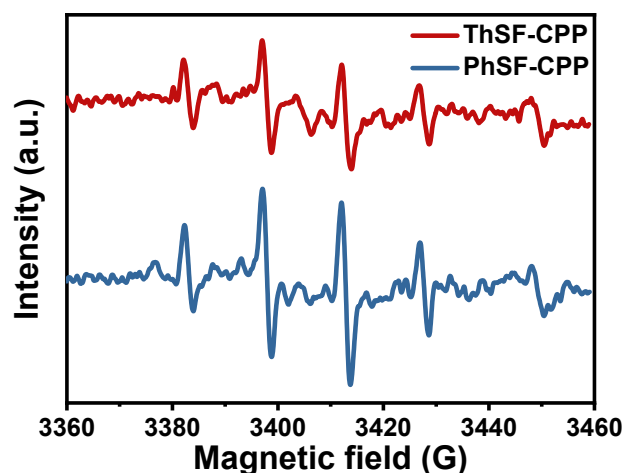


Fig. S17. EPR spectra of detecting DMPO-·OH of ThSF-CPP and PhSF-CPP under light irradiation.

References

- [1] M.J. Frisch, G.W. Trucks, H.B. Schlegel, G.E. Scuseria, M. A. Robb, J.R. Cheeseman, G. Scalmani, V. Barone, G.A. Petersson, H. Nakatsuji, X. Li, M. Caricato, A.V. Marenich, J. Bloino, B.G. Janesko, R. Gomperts, B. Mennucci, H.P. Hratchian, J.V. Ortiz, A.F. Izmaylov, J.L. Sonnenberg, D. Williams-Young, F. Ding, F. Lipparini, F. Egidi, J. Goings, B. Peng, A. Petrone, T. Henderson, D. Ranasinghe, V.G. Zakrzewski, J. Gao, N. Rega, G. Zheng, W. Liang, M. Hada, M. Ehara, K. Toyota, R. Fukuda, J. Hasegawa, M. Ishida, T. Nakajima, Y. Honda, O. Kitao, H. Nakai, T. Vreven, K. Throssell, J.A. Montgomery, Jr., J.E. Peralta, F. Ogliaro, M.J. Bearpark, J.J. Heyd, E.N. Brothers, K.N. Kudin, V.N. Staroverov, T.A. Keith, R. Kobayashi, J. Normand, K. Raghavachari, A.P. Rendell, J.C. Burant, S.S. Iyengar, J. Tomasi, M. Cossi, J.M. Millam, M. Klene, C. Adamo, R. Cammi, J.W. Ochterski, R.L. Martin, K. Morokuma, O. Farkas, J.B. Foresman, and D.J. Fox, Gaussian, Inc., Wallingford CT, Gaussian 16, Revision C.01, 2016.
- [2] G. Kresse, J. Furthmüller, Efficient iterative schemes for ab initio total-energy calculations using a plane-wave basis set, *Phys. Rev. B.* 54 (1996) 11169-11186.
- [3] G. Kresse, D. Joubert, From ultrasoft pseudopotentials to the projector augmented-wave method, *Phys. Rev. B.* 59 (1999) 1758-1775.
- [4] P. Perdew, K. Burke, M. Ernzerhof, Generalized gradient approximation made Simple, *Phys. Rev. Lett.* 77 (1996) 3865-3868.
- [5] T. Lu, F. Chen, Multiwfn: A multifunctional wavefunction analyzer, *J Comput Chem* 33 (2012) 580-592.
- [6] W. Humphrey, A. Dalke, K. Schulten, VMD: visual molecular dynamics, *J. Mol. Graph* 14 (1996) 33-38.
- [7] X. Han, F. Zhao, Q.Q. Shang, J.S. Zhao, X.J. Zhong, J.H. Zhang, Effect of nitrogen atom introduction on the photocatalytic hydrogen evolution activity of covalent triazine frameworks: experimental and theoretical study, *ChemSusChem* 15 (2022) e202200828.
- [8] R.S. Sprick, B. Bonillo, M. Sachs, R. Clowes, J.R. Durrant, D.J. Adams, A.I. Cooper, Extended conjugated microporous polymers for photocatalytic hydrogen evolution from water, *Chem. Comm.* 52 (2016) 10008-10011.
- [9] R.S. Sprick, Y. Bai, A.A.Y. Guilbert, M. Zbiri, C.M. Aitchison, L. Wilbraham, Y. Yan, D.J. Woods,

- M.A. Zwijnenburg, A.I. Cooper, Photocatalytic hydrogen evolution from water using fluorene and dibenzothiophene sulfone-conjugated microporous and linear polymers, *Chem. Mater.* 31 (2019) 305-313.
- [10] F.L. Yi, Q. Yang, X.Y. Li, Y.Q. Yuan, H.M. Cao, K.W. Liu, H.J. Yan, A 1, 3, 5-triazine and benzodithiophene based donor-acceptor type semiconducting conjugated polymer for photocatalytic overall water splitting, *J Solid State Chem* 318 (2023) 123769.
- [11] L.J. Liu, M.A. Kochman, Y.J. Xu, M.A. Zwijnenburg, A.I. Cooper, R.S. Sprick, Acetylene-linked conjugated polymers for sacrificial photocatalytic hydrogen evolution from water, *J. Mater. Chem. A* 9 (2021) 17242-17248.
- [12] A.M. Elewa, A.F. EL-Mahdy, M.H. Elsayed, M.G. Mohamed, S.W. Kuo, H.H. Chou, Sulfur-doped triazine-conjugated microporous polymers for achieving the robust visible-light-driven hydrogen evolution, *Chem. Eng. J.* 421 (2021) 129825.
- [13] Y.C. Yan, X.H. Yu, C.C. Shao, Y.P. Hu, W. Huang, Y.G. Li, Atomistic structural engineering of conjugated microporous polymers promotes photocatalytic biomass valorization, *Adv. Funct. Mater.* (2023) 2304604.
- [14] Y.S. Kochergin, D. Schwarz, A. Acharjya, A. Ichangi, R. Kulkarni, P. Eliášová, J. Vacek, J. Schmidt, A. Thomas, M.J. Bojdys, Exploring the “goldilocks zone” of semiconducting polymer photocatalysts by donor-acceptor interactions, *Angew. Chem. Int. Ed.* 57 (2018) 14188-14192.
- [15] G.H. Zhang, A.M. Elewa, M. Rashad, S. Helali, H.H. Chou, A.F. EL-Mahdy, Triazine-and porphyrin-based donor-acceptor microporous conjugated polymers for enhanced photocatalytic hydrogen production activity, *Microporous Mesoporous Mater.* 363 (2024) 112824.